AMERICAN SOCIETY FOR MICROBIOLOGY | Molecular and Cellular Biology®

RESEARCH ARTICLE

Unexpected Role of Matrix Gla Protein in Osteoclasts: Inhibiting Osteoclast Differentiation and Bone Resorption

Yan Zhang,[a] Liting Zhao,[a] Naining Wang,[a,b] Jing Li,[a] Fang He,[a] Xu Li,[a] Shufang Wu[a]

[a]Center for Translational Medicine, The First Affiliated Hospital of Xi'an Jiaotong University, Xi'an, Shaanxi, People's Republic of China
[b]The Key Laboratory of Biomedical Information Engineering of the Ministry of Education, Xi'an Jiaotong University, Xi'an, Shaanxi, People's Republic of China

ABSTRACT Matrix Gla protein (MGP) is an extracellular protein responsible for inhibiting mineralization. MGP inhibits osteoblast mineralization and bone formation by regulating the deposition of bone matrix. However, *Mgp*$^{-/-}$ mice display an osteopenic phenotype. To explain this contradiction, we investigated the role of MGP in osteoclastogenesis, the other side of bone remodeling. We found that MGP expression is markedly increased by osteoclastic commitment. Osteoclast differentiation and bone resorption are accelerated by MGP depletion while suppressed by MGP overexpression. The *in vivo* results confirmed its inhibitory role in osteoclastogenesis by the administration of Cre-dependent FLEX-On recombinant MGP-AAV to LysM Cre mice. Furthermore, we found that the expression and nuclear translocation of nuclear factor of activated T cells, cytoplasmic 1 (NFATc1), are under the control of MGP. MGP loss results in elevation of intracellular Ca^{2+} flux. Vitronectin-induced activation of Src/Rac1 is magnified in the absence of MGP but reduced when MGP is overexpressed. Inhibition of Src activation or NFATc1 nuclear import rescues the increased osteoclastogenesis induced by MGP deficiency. These observations (i) establish, for the first time to our knowledge, that MGP plays an essential role in osteoclast differentiation and function, (ii) enrich the current knowledge of MGP function, and (iii) indicate the potential of MGP as a therapeutic target for low-bone-mass disorders.

KEYWORDS MGP, bone loss, osteoclast differentiation, osteoclastogenesis

Matrix Gla protein (MGP) is a 14-kDa secreted extracellular protein that is initially extracted and purified from demineralized bone. MGP belongs to the mineral binding protein family and is known as a potent inhibitor of mineralization (1). Mice deficient in *Mgp* show severe vascular calcification and premature bone mineralization and die in the first weeks of their lives (2). The gamma-glutamate (Gla) residues of MGP, which are produced posttranslationally by a vitamin K-dependent carboxylation reaction of glutamyl residues, have high affinity for calcium, phosphate ions, and hydroxyapatite. The Gla residues are critical for the function of MGP (3). If these residues are not modified properly (no Gla present), there will be a risk of osteoporosis and vascular calcification in human patients undergoing anticoagulant therapy (4).

Transgenic mice overexpressing *Mgp* in osteoblasts, under the control of the 2.3-kb α1(I)-collagen gene promoter, exhibit decrease in intramembranous bone mineralization, and most of their tooth dentin and cementum are hypomineralized, suggesting that MGP grossly disrupts bone formation (5). It has been reported that inflammatory arthritis patients had significantly higher inactive uncarboxylated MGP levels in synovial fluid compared to controls, implying a potential role of MGP in arthritis (6). Genetic *Mgp* polymorphism is also associated with osteoarthritis and low bone mineral density (7, 8). Retrovirus-mediated overexpression of MGP in developing growth plates impairs endochondral ossification by delaying chondrocyte differentiation (9). Inhibition of MGP

Citation Zhang Y, Zhao L, Wang N, Li J, He F, Li X, Wu S. 2019. Unexpected role of matrix Gla protein in osteoclasts: inhibiting osteoclast differentiation and bone resorption. Mol Cell Biol 39:e00012-19. https://doi.org/10.1128/MCB.00012-19.

Address correspondence to Xu Li, lixuxjtu@163.com, or Shufang Wu, shufangw@hotmail.com.

Received 27 February 2019
Returned for modification 12 March 2019
Accepted 8 April 2019
Accepted manuscript posted online 15 April 2019
Published 28 May 2019

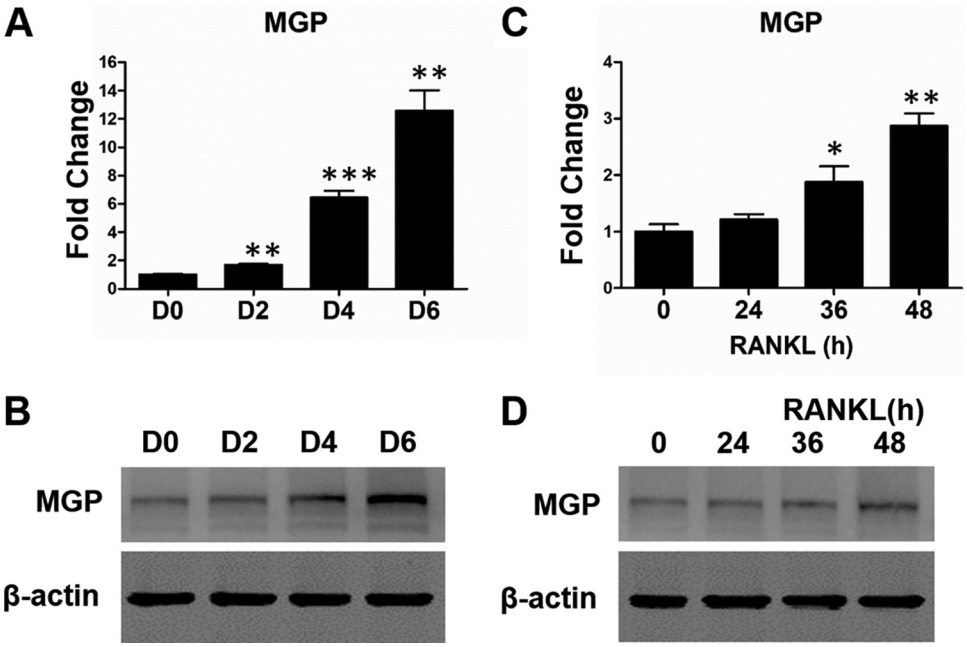

FIG 1 Expression profile of MGP during osteoclast differentiation. (A) mRNA analysis of MGP during osteoclast differentiation. BMMs were induced with 30 ng/ml M-CSF and 100 ng/ml RANKL for 6 days before being harvested for mRNA detection using qPCR. (B) Immunoblot analysis of MGP during osteoclast differentiation. BMMs were induced with 30 ng/ml M-CSF and 100 ng/ml RANKL for 6 days. The cells were then harvested at the indicated time points for Western blotting. (C) MGP mRNA analysis of RAW 264.7 cells. RAW 264.7 cells were treated with 100 ng/ml RANKL for the indicated times before being harvested for mRNA analysis. (D) Immunoblot analysis of MGP expression in RAW 264.7 cells. The treatment was as described for panel C. *, $P < 0.05$; **, $P < 0.01$; ***, $P < 0.001$.

function leads to considerable reduction of parathyroid hormone (PTH)-inhibited osteoblast mineralization, suggesting a role for MGP in osteoblastogenesis (10).

An important factor in the maintenance of bone mass is osteoclast-mediated bone resorption. Osteoclast differentiation is initiated by macrophage colony-stimulating factor (M-CSF) and receptor activator of nuclear factor-κB ligand (RANKL) (11). RANKL-induced signaling cascades activate the nuclear factor of activated T cells, cytoplasmic 1 (NFATc1), which is the key transcriptional factor in osteoclastogenesis. Calcium (Ca^{2+}) oscillation, the release of Ca^{2+} from the endoplasmic reticulum, and the consequent influx of Ca^{2+} from the extracellular milieu are essential for the nuclear translocation and activation of NFATc1 (12).

The function of MGP has been significantly associated with bone phenotype. Lots of studies suggested its role in chondrocytes and osteoblasts (13, 14). However, until now there has been no report indicating a role of MGP in osteoclastogenesis. Moreover, Marulanda et al. reported that the transgenic overexpression of MGP in vascular smooth muscle cells (VSMCs) rescues the low-bone-mass phenotype in *Mgp* knockout mice, suggesting that arterial calcification, not MGP deficiency itself, causes the low-bone-mass phenotype (15). In the present study, we examined the function of MGP in the differentiation of osteoclast. We suggest that MGP inhibits osteoclastogenesis *in vitro* and *in vivo*. Our results prove that MGP itself has a direct role in bone homeostasis, especially in the regulation of osteoclast formation and function.

RESULTS

MGP deficiency stimulates osteoclast formation and function. We first detected the expression profile of MGP in response to differentiation-inducing stimuli. Bone marrow macrophages (BMMs) were cultured in the presence of M-CSF and RANKL to promote osteoclastogenesis. As shown in Fig. 1A and B, MGP expression was significantly increased during osteoclastogenesis. A similar MGP induction effect was also

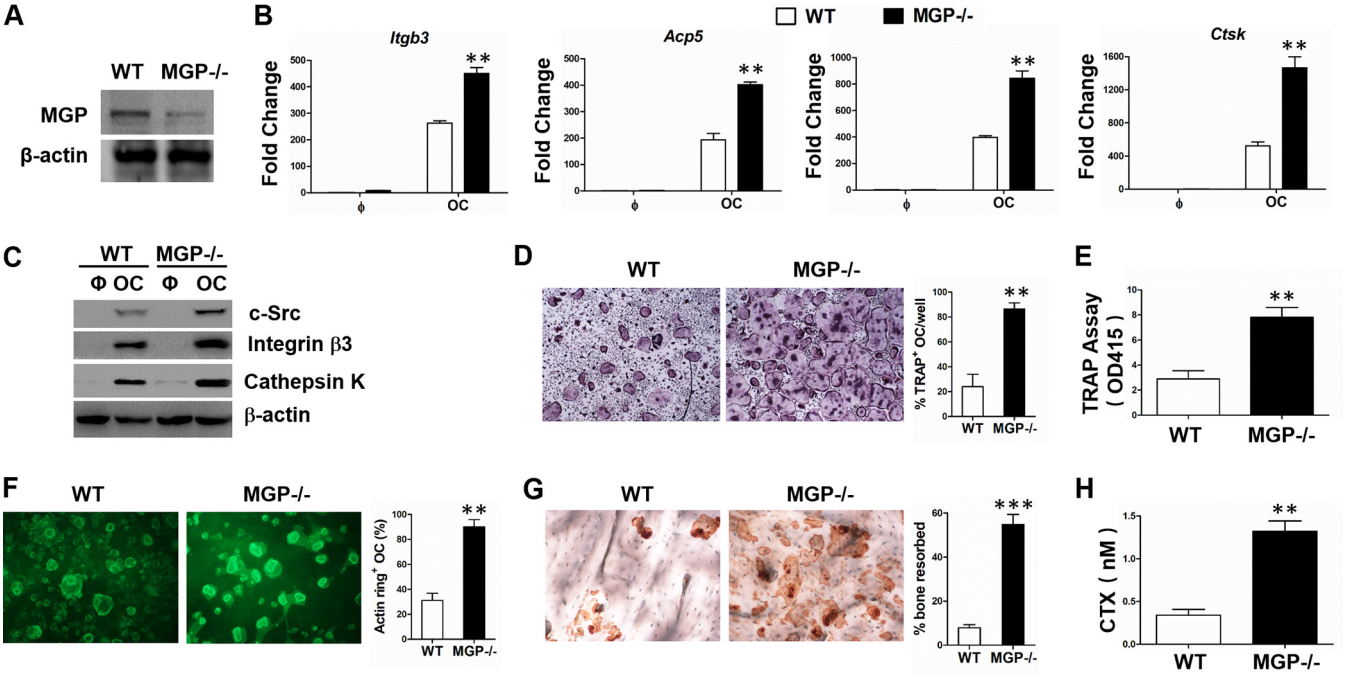

FIG 2 MGP depletion stimulates osteoclast differentiation and activity. (A) Efficiency of MGP knockout in BMMs using a CRISPR-Cas9 system. (B) Knockout of MGP leads to an increase in the mRNA levels of osteoclastic markers. BMMs were induced with 30 ng/ml M-CSF and 100 ng/ml RANKL for 4 days before being harvested for mRNA analysis. (C) Immunoblot analysis of osteoclastic marker expression. BMMs were induced with 30 ng/ml M-CSF and 100 ng/ml RANKL for 4 days before being harvested for Western blotting. (D) MGP deficiency promotes the formation of mature osteoclasts. BMMs were induced with 30 ng/ml M-CSF and 100 ng/ml RANKL for 3 days. The cells were then fixed and stained with TRAP solution, and the TRAP-positive multinucleated cells were counted. (E) MGP deficiency increases TRAP activity. BMMs were induced with 30 ng/ml M-CSF and 100 ng/ml RANKL for 3 days. The cells were then lysed, and medium TRAP activity was determined by TRAP assay. (F) MGP deficiency increases actin ring formation of osteoclasts. BMMs were cultured on bone slices with 30 ng/ml M-CSF and 100 ng/ml RANKL for 4 days. The cells were then fixed and stained with FITC-phalloidin. The actin-ring-positive osteoclasts were counted. (G) MGP deficiency increases osteoclast-mediated bone resorption. BMMs were cultured on bone slices with 30 ng/ml M-CSF and 100 ng/ml RANKL for 4 days. The cells were removed, and resorption pits were stained with peroxidase-conjugated wheat germ agglutinin. The pits were then counted. (H) MGP depletion stimulates the release of CTX. BMMs were cultured on bone slices with 30 ng/ml M-CSF and 100 ng/ml RANKL for 4 days. The culture supernatant was collected and assayed to determine the amount of CTX. **, $P < 0.01$; ***, $P < 0.001$.

observed in RANKL-treated RAW 264.7 cells (Fig. 1C and D). We then generated BMMs with the MGP depletion (MGP-deleted BMMs) using the CRISPR-Cas9 system in which the gene is deleted at least 80% (Fig. 2A). As shown in Fig. 2B, the osteoclastic maker genes in MGP-deficient cells, including the integrin β3 (*Itgb3*), TRAP5 (*Acp5*), DC-STAMP (*Dcst1*), and cathepsin K (*CtsK*) genes, are induced with a much greater magnitude compared to controls. Consistently, immunoblot results also confirmed the elevated protein expression of these markers and c-Src, an important osteoclastic signaling mediator (Fig. 2C). MGP-deficient BMMs form many more tartrate-resistant acid phosphatase (TRAP)-positive osteoclasts, and the cells are much bigger compared to the control (Fig. 2D). The TRAP assay also confirmed the significantly increased TRAP staining (Fig. 2E). To determine the osteoclast function after MGP was deleted, BMMs were seeded on the bone slices and induced for 4 days, and actin ring formation assays were performed. As shown in Fig. 2F, compared to controls, the MGP-deleted cells form many more actin rings. There were significantly more pits formed by the MGP-deleted cells (Fig. 2G). CTX (C-terminal telopeptide type I collagen) levels, a marker of bone matrix degradation, in the culture medium were examined. The concentration of CTX from the MGP-deficient cells is significantly higher than that of control cells (Fig. 2H).

MGP overexpression retards osteoclast formation and function. Then we overexpressed MGP in BMMs using recombinant retrovirus and detected the effects of MGP overexpression on osteoclastogenesis. The overexpression efficiency was validated by Western blotting (Fig. 3A). Consistent with the knockout results, MGP overexpression led to inhibited expression of osteoclast differentiation makers, as indicated by the decreased mRNA levels (Fig. 3B) and decreased protein levels (Fig. 3C). After 4 days of

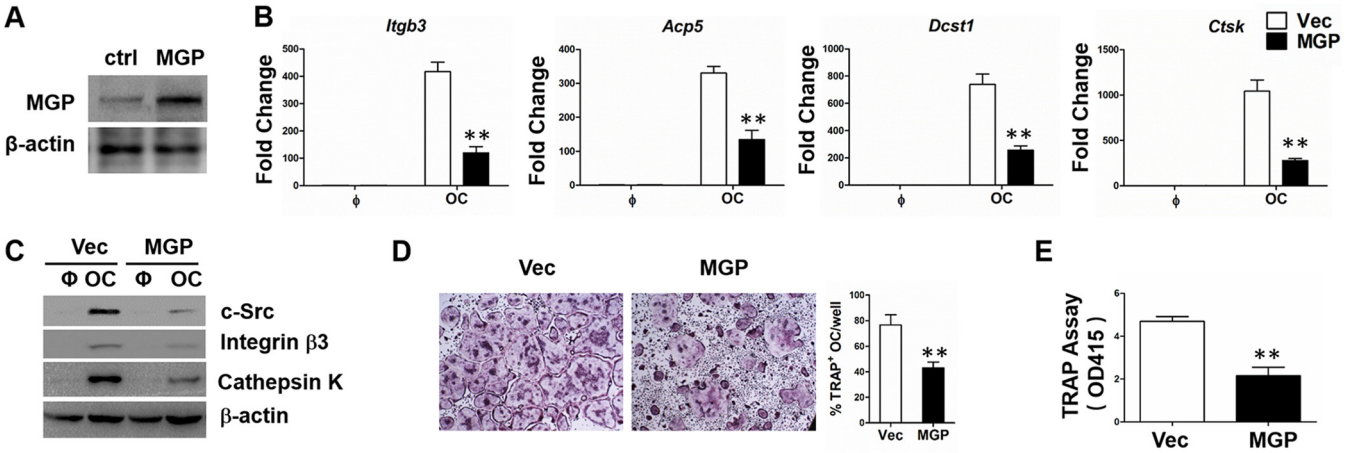

FIG 3 Overexpression of MGP suppresses osteoclast differentiation. (A) Efficiency of MGP overexpression in BMMs. (B) Overexpression of MGP decreases the mRNA levels of osteoclastic markers. BMMs were induced with 30 ng/ml M-CSF and 100 ng/ml RANKL for 4 days before being harvested for mRNA analysis. (C) Immunoblot analysis of osteoclastic markers expression during osteoclast differentiation. The treatments are as described for panel B. (D) MGP overexpression inhibits the formation of mature osteoclasts. BMMs were induced with 30 ng/ml M-CSF and 100 ng/ml RANKL for 4 days. The cells were then fixed and stained with TRAP solution, and TRAP-positive multinucleated cells were counted. (E) MGP overexpression decreases the TRAP activity. BMMs were induced with 30 ng/ml M-CSF and 100 ng/ml RANKL for 4 days. The cells were then lysed, and the medium TRAP activity was determined by a TRAP assay. **, $P < 0.01$.

induction, the number of TRAP-positive osteoclasts was significantly lower than the number of control cells (Fig. 3D). TRAP assays also confirmed the impaired TRAP staining (Fig. 3E).

AAV-mediated MGP overexpression increases bone mass via suppressing osteoclastogenesis. To confirm the role of MGP *in vivo*, we used a Cre-dependent FLEX-On AAV-mediated gene transduction strategy to overexpress MGP in osteoclastic cells and examine the effects *in vivo*. LysM Cre mice were intratibially injected with Cre-dependent MPG recombinant AAV or control AAV. The FLEX-On AAV recombinant vector contains reverse mouse MGP cDNA flanked by two oppositely orientated loxP sites. The expression of MGP is turned on in Cre-expressing cells (myeloid lineage cells, osteoclast precursor) (Fig. 4A). This strategy makes MGP specifically overexpressed in osteoclast precursors. Eight weeks later, bones were collected for histological and microcomputed tomography (μCT) analysis. The overexpression efficiency was validated in Fig. 4B. As shown in Fig. 4C, TRAP staining demonstrated that MGP-overexpressing mice have far fewer osteoclasts than do control mice. The percentage of osteoclast surface to bone surface in MGP-overexpressing mice is significantly decreased compared to controls. μCT analysis indicated that the bone mass of MGP-overexpressing mice is significantly elevated. Consistently, the bone volume/total volume (BV/TV) ratio, the trabecular number (Tb.No.), and the trabecular thickness (Tb.Th.) are significantly increased, whereas the trabecular spacing (Tb.Sp.) is dramatically decreased (Fig. 4D). Serum TRAP5b, an indicator of osteoclast number, is significantly decreased in MGP-overexpressing mice (Fig. 4E). Calcein double labeling showed that the periosteum in the tibias of the MGP-overexpressing mice exhibited no difference in the mineral apposition rate compared to the control, indicating no change in osteoblast activity (Fig. 4F). Moreover, serum osteocalcin (OCN), an indicator of osteoblast activity and bone formation, remained unchanged (Fig. 4G).

MGP regulates NFATc1 cellular localization. To reveal the molecular mechanism underlying MGP-mediated control of osteoclast differentiation and function, we detected the expression of NFATc1, which is the key transcriptional factor in osteoclastogenesis. As shown in Fig. 5A, the mRNA levels of NFATc1 in MGP-depleted osteoclasts is significantly higher compared to control cells. In contrast, NFATc1 mRNA expression is dramatically inhibited in MGP-overexpressing cells during osteoclast differentiation (Fig. 5B). Consistent with the mRNA results, NFATc1 protein levels are also stimulated by MGP depletion and suppressed by MGP overexpression. Particularly, MGP deficiency

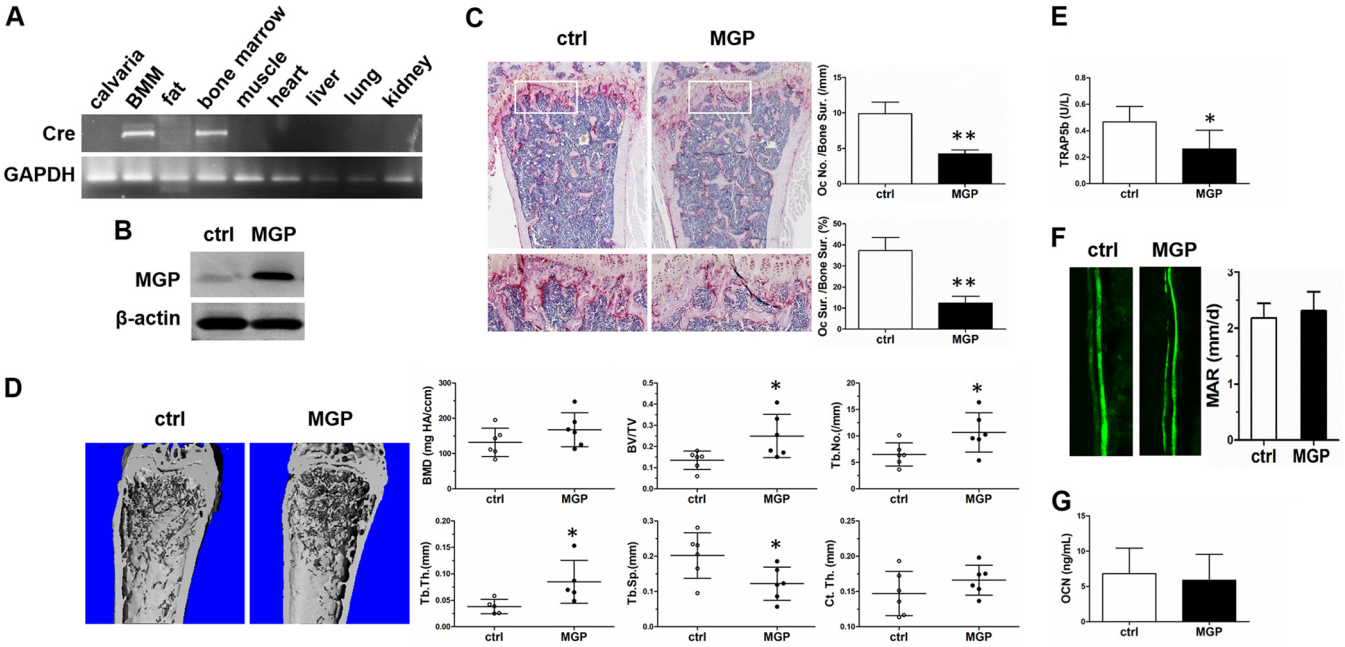

FIG 4 MGP suppresses osteoclastogenesis *in vivo*. (A) Confirmation of Cre expression in different cells and tissues. (B) Eight-week-old LysM Cre male mice were intratibially injected with recombinant MGP AAV (2×10^{11} vg) or control rAAV. After 8 weeks, the mice were sacrificed, and samples were collected. MGP overexpression in the BMMs was confirmed by Western blotting. (C) Histology analysis of the femur. Sections of femurs were stained for TRAP activity. (D) Microcomputed tomography (μCT) analyses of the trabecular bone in the distal femur. Bone morphometric analysis of the osteoblastic parameters was also performed. (E) Enzyme-linked immunosorbent assay (ELISA) of the serum levels of osteoclast number marker TRAP5b. (F) Representative images of double labeling and dynamic histomorphometric parameter in the periosteum in the tibia. (G) ELISA of the serum level of bone formation marker OCN. The data are means ± the standard deviations from six mice. *, $P < 0.05$; **, $P < 0.01$.

promotes NFATc1 nuclear translocation in response to RANKL induction, whereas MGP ectopically expression retains NFATc1 in the cytoplasm compared to the control cells (Fig. 5C). Altogether, these data indicate that MGP acts as a negative regulator to restrain NFATc1 activation during osteoclastogenesis.

MGP moderates intracellular calcium mobilization. RANKL induced the rise in cytoplasmic calcium (Ca^{2+}), which in turn triggers Ca^{2+}/calmodulin-dependent NFATc1 expression and nuclear translocation. We detected the intracellular Ca^{2+} concentration to see whether it is affected after MGP expression is modified. As expected, the cellular Ca^{2+} flux detected by Fluo-2 is increased after RANKL is added in the control RAW 264.7 cells (Fig. 6A). Although the basal levels of Ca^{2+} concentration are indistinguishable between control RAW 264.7 cells and MGP-depleted RAW 264.7 cells, the increased amplitude of RANKL-induced Ca^{2+} concentration in the MGP-depleted cells is much greater than in control cells (Fig. 6A to C). These results demonstrated that MGP modulates Ca^{2+} fluxes in osteoclasts.

MGP regulates activation of Src/Rac1 signaling. Activation of Src and Rac1 is the canonical signaling involved in osteoclast differentiation. To determine whether the stimulated osteoclast differentiation attending MGP deletion reflects activation of the canonical pathway, we assessed the activation state of Src and Rac1 upon integrin stimulation. We used vitronectin which contains the RGD motif to activate $\alpha v\beta 3$ integrin, the principal Src/Rac1-inducing integrin in osteoclasts. As expected, $\alpha v\beta 3$ stimulation activated Src, as manifested by S416 phosphorylation in control preosteoclasts (Fig. 7A). However, the phosphorylation of Src is obviously elevated in MGP-depleted preosteoclasts, while it is dramatically reduced in MGP-overexpressing preosteoclasts in comparison to control cells (Fig. 7A). The activation of Rac1 as manifested by GTP association was then detected. As shown in Fig. 7B, vitronectin stimulation yielded Rac1 activation effects similar to those of Src in mutant cells. Therefore, MGP modulates osteoclast differentiation in a Src/Rac1 signaling-dependent manner. To further confirm the involvement of Src/Rac signaling in the effects of MGP, the Src

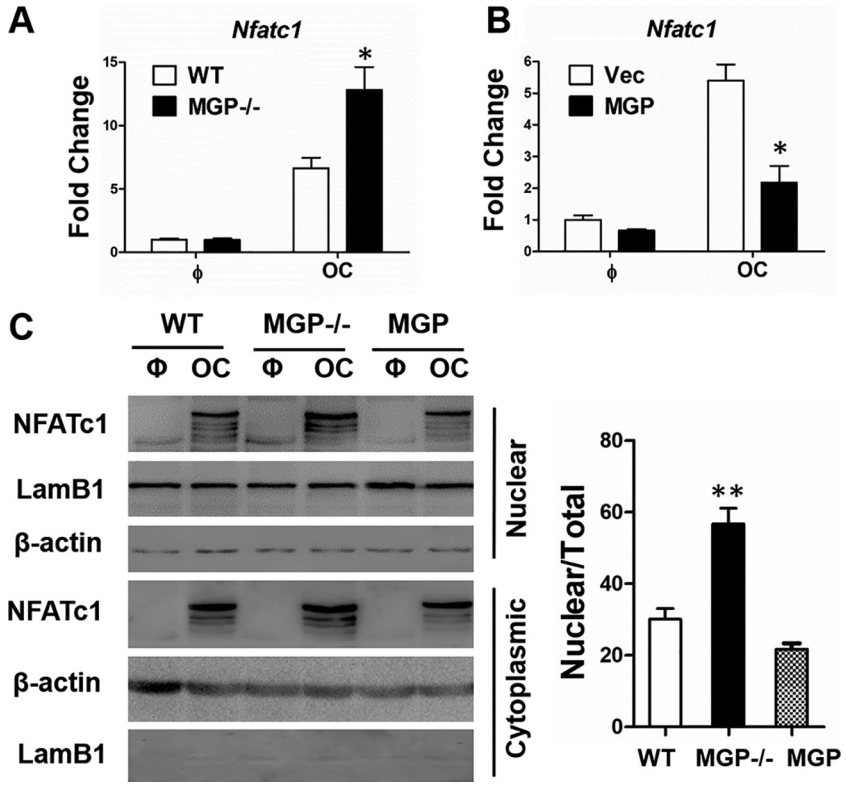

FIG 5 MGP controls the expression and nuclear translocation of NFATc1. (A) Knockout of MGP leads to an increase in the NFATc1 mRNA level. BMMs were induced with 30 ng/ml M-CSF and 100 ng/ml RANKL for 4 days. Cells were harvested for mRNA analysis. (B) Overexpression of MGP decreases the NFATc1 mRNA level. The treatment was as described for panel A. (C) MGP modulates the nuclear translocation of NFATc1. BMMs were induced with 30 ng/ml M-CSF and 100 ng/ml RANKL for 4 days. The cells were harvested, and the nuclear/cytoplasmic fractions were separated for immunoblot analysis. *, $P < 0.05$; **, $P < 0.01$.

inhibitor KX2-391 or the NFATc1 inhibitor INCA-6 was used during the culture of osteoclasts. As expected, Src inhibition rescues the increased osteoclastogenesis induced by MGP deficiency, as shown by TRAP staining (Fig. 7C) and the mRNA levels of osteoclastic markers (Fig. 7D). Consistently, in the presence of the NFATc1 inhibitor INCA-6, MGP deficiency-induced osteoclastogenesis is rescued (Fig. 7E and F). Furthermore, we collected the BMMs from the rAAV-injected mice and detected Src/Rac1 signaling. Src phosphorylation and Rac1 activation is inhibited in the MGP-overexpressing preosteoclasts (Fig. 7G). Collectively, our data confirm the involvement of NFATc1 and Src/Rac1 signaling in the MGP's effect on osteoclastogenesis.

DISCUSSION

Bone remodeling involves osteoblast-mediated bone formation and osteoclast-mediated bone resorption. Imbalance of bone remodeling leads to low-bone-mass disorders such as osteoporosis (16). Therapeutic regulation of osteoclast may represent an important method to maintain the bone mass in these disorders. Vascular calcification, a chronic degenerative cardiovascular disorder, has been increasingly associated with bone loss, and vascular calcification and bone loss might share common pathogenetic mechanisms involving MGP (17).

Marulanda et al. observed that the low-bone-mass phenotype in *Mgp*$^{-/-}$ mice was rescued by transgenic overexpression of *Mgp* in the VSMCs, indicating the indirect role of MGP derived from vascular system in bone homeostasis (15). This observation provides a possible relation between bone loss and vascular calcification. However, it cannot exclude the possibility that MGP *per se* has a direct role in bone remodeling. In addition, *Mgp*$^{-/-}$ mice show osteopenic phenotype but with enhancement of alkaline

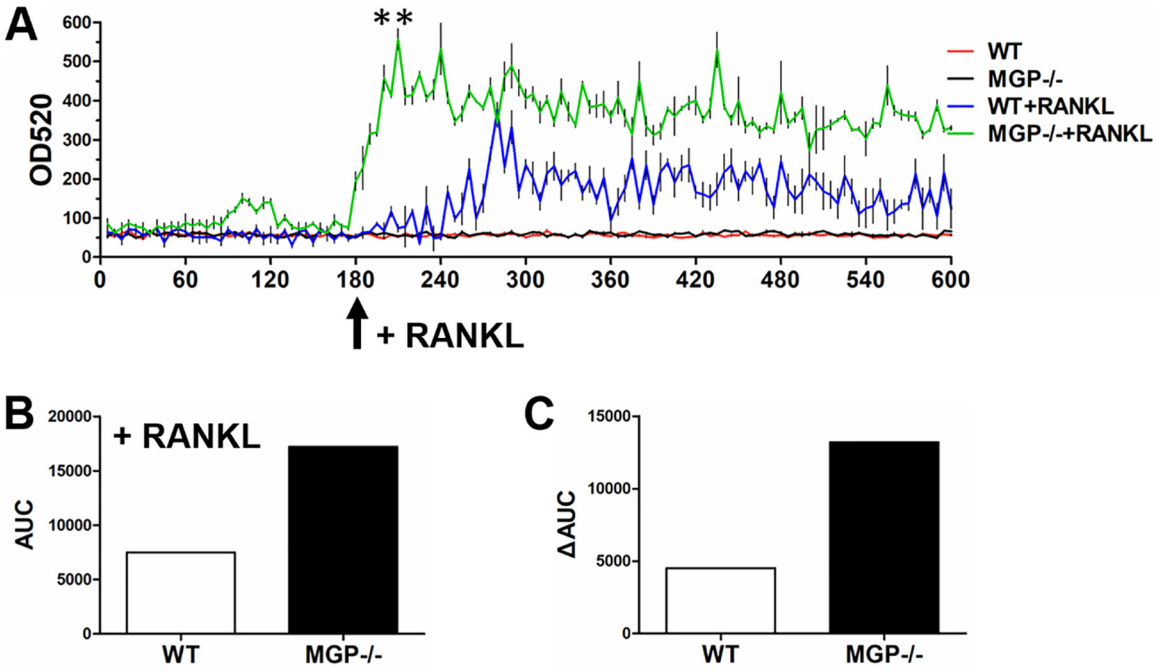

FIG 6 MGP modulates intracellular calcium mobilization. (A) Cytosolic Ca^{2+} measurements in the absence or presence of 100 ng/ml RANKL. Wild-type or MGP$^{-/-}$ RAW 264.7 cells were loaded with Fluo-2 before the absorbance was detected by excitation at 488 nm and emission at 520 nm every 5 s for 10 min. RANKL was added at the indicated time point. Each condition was examined using three replicates. (**, $P < 0.01$). (B) Areas under the curve (AUC) for the WT+RANKL and MGP$^{-/-}$+RANKL cells in panel A. WT, wild type. (C) Difference in AUC after RANKL treatment in wild-type and MGP$^{-/-}$ cells. **, $P < 0.01$.

phosphatase (ALP) activity and increased expression of osteoblastic genes in bone (18). This seems contradictory and prompted us to investigate the role of MGP in osteoclastogenesis.

Here, we observed that MGP expression is markedly increased by osteoclastic commitment. Osteoclast differentiation and bone resorption are accelerated by MGP depletion but suppressed by MGP overexpression. *In vivo* results confirmed the inhibitory role of MGP in osteoclastogenesis by the administration of recombinant AAV. Furthermore, the expression and nuclear translocation of NFATc1 is under the control of MGP. Interestingly, MGP loss results in the elevation of intracellular Ca^{2+} flux. Vitronectin induced activation of Src and Rac1 is significantly magnified in the absence of MGP but reduced when MGP is overexpressed. The underlying mechanism is MGP attenuates the integrin-induced activation of Src/Rac1 canonical pathway, as well as interfering with the Ca^{2+} flux induction of NFATc1 activation. These observations establish for the first time that MGP plays an essential role in osteoclast differentiation and function, enrich the current knowledge of MGP function, and indicate the potential of MGP as a therapeutic target for low-bone-mass disorders.

MGP is induced significantly in the presence of RANKL, despite further evidence show that MGP inhibits osteoclast differentiation and formation. We speculate that at the late stage of osteoclast differentiation, MGP is highly expressed to avoid overstimulation of osteoclast formation, causing a negative-feedback loop to make osteoclast formation under delicate control. Unexpectedly, the MGP-depleted BMMs differentiate into mature osteoclasts at day 3 *in vitro*, which is much earlier than their wild-type counterparts under our regular culture conditions, which normally takes 5 or 6 days. This finding implies that MGP may act at an early stage of osteoclast differentiation, when it is actually not abundant. The activity of MGP may change immediately in response to osteoclastic stimuli.

Integrin mediates outside-in osteoclastic signaling involving c-Src, Dap12, Vav3, and Rac (19). Our data show that MGP regulates the vitronectin induction of Src phosphor-

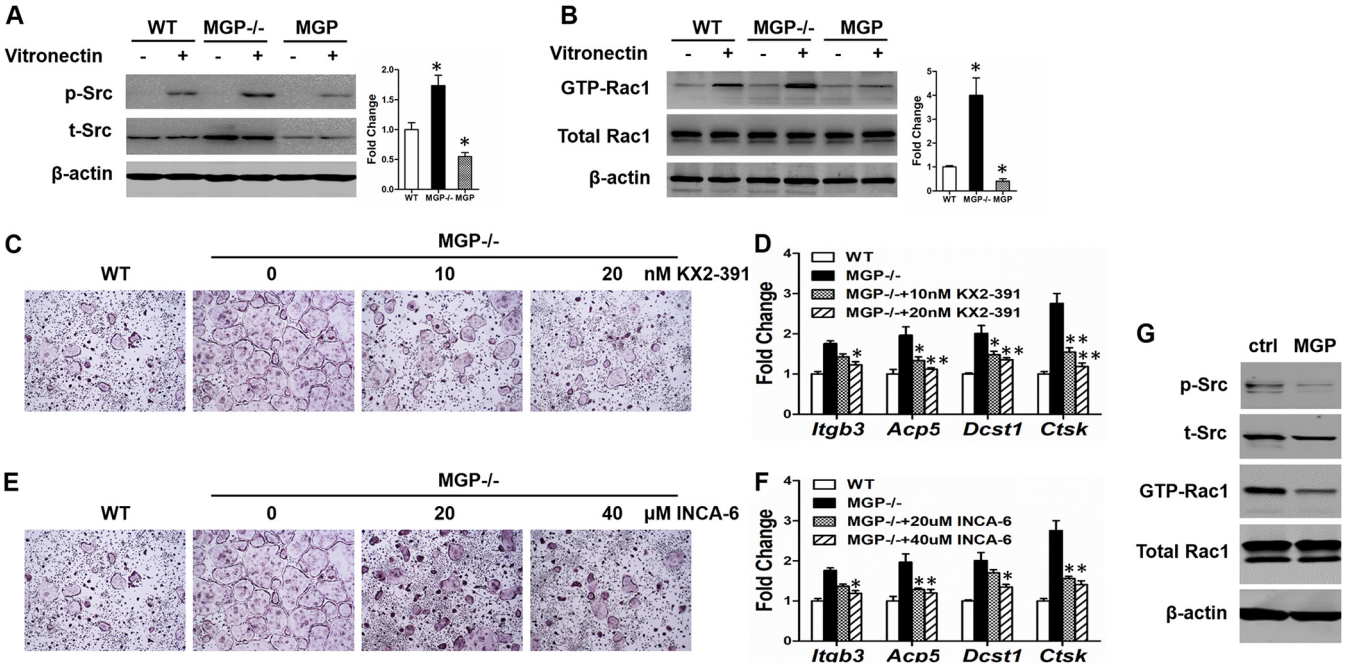

FIG 7 MGP modulates Src-Rac canonical signaling. (A) MGP regulates Src activation upon vitronectin stimulation. Preosteoclasts were starved in serum-free medium for 3 h before being plated on vitronectin-coated plates or maintained in suspension for 30 min. An immunoblot analysis was then conducted to detect the activation of Src. (B) MGP regulates Rac1 activation upon vitronectin stimulation. Preosteoclasts were starved in serum-free medium overnight before being plated on vitronectin-coated plates or maintained in suspension for 30 min. A pulldown assay and immunoblot analysis were then conducted. (C) BMMs were induced with 30 ng/ml M-CSF and 100 ng/ml RANKL for 3 days. KX2-391 (an Src inhibitor) was also added to $MGP^{-/-}$ BMMs at the indicated concentrations. The cells were then fixed and stained with TRAP solution. (D) BMMs were induced with 30 ng/ml M-CSF and 100 ng/ml RANKL for 4 days before being harvested for mRNA analysis. KX2-391 was also added in the $MGP^{-/-}$ BMMs at the indicated concentrations. (E) BMMs were induced with 30 ng/ml M-CSF and 100 ng/ml RANKL for 3 days. INCA-6 (an NFATc1 inhibitor) was also added to $MGP^{-/-}$ BMMs at the indicated concentrations. The cells were then fixed and stained with TRAP solution. (F) BMMs were induced with 30 ng/ml M-CSF and 100 ng/ml RANKL for 4 days before being harvested for mRNA analysis. INCA-6 was also added to $MGP^{-/-}$ BMMs at the indicated concentrations. (G) Src and Rac signaling is attenuated during rAAV-mediated MGP overexpression in LysM Cre mice. The BMMs were harvested from the rAAV-injected mice, and Src/Rac signaling was detected as described in the text. *, $P < 0.05$; **, $P < 0.01$.

ylation and GTP-Rac1. It has been reported that MGP could bind with vitronectin and other extracellular matrix proteins (20). Therefore, we speculated that MGP interferes with vitronectin-induced signaling, probably by blocking vitronectin and inhibiting the activation of integrin. In addition, our results demonstrated that MGP inhibits the expression of β3 integrin. Regulation of the abundance and activation status of β3 integrin is an underlying mechanism of MGP function in osteoclast function in addition to the control of Ca^{2+} mobilization. Which one is dominating needs to be further studied.

Lots of studies have reported the role of MGP in osteoblast differentiation and mineralization. MGP inhibits osteoblast mineralization and affects bone mass by regulating the deposition of the bone matrix (13, 14). We found that the osteoclast number is controlled by MGP, reflecting the inhibitory role of MGP in osteoclastogenesis. This may explain the contradictory phenotype of *Mgp*$^{-/-}$ mice between the osteopenic phenotype and the accelerated mineralization and osteoblast differentiation, that is, the concomitant increase in bone resorption exceeds that of bone formation.

MGP is mainly synthesized by chondrocytes, osteoblasts, and osteocytes in bone (21). This may be why people ignored MGP in osteoclasts for a long time. Although the expression level of MGP in mature osteoclast is not abundant, its role in osteoclastogenesis is surprisingly significant. However, we only investigated endogenous MGP in osteoclasts. As a secreted protein, the extracellular MGP produced by other cells, such as osteoblasts and chondrocytes, may also play roles in the cross talk of osteoclasts and these cells. This needs to be investigated more fully in the near future.

Collectively, we report for the first time, to our knowledge, that MGP plays an inhibitory role in osteoclast differentiation and function. The molecular evidence

indicates that MGP controls osteoclastogenesis via modulation of the intracellular calcium flux and Src/Rac1 signaling. Our observation enriches the current knowledge of MGP function and indicates the potential of MGP as a therapeutic target for low-bone-mass disorders in the future.

MATERIALS AND METHODS

***In vitro* osteoclastogenesis.** Mouse BMMs were prepared as previously described (22). Briefly, marrow extracted from femora and tibias of 6- to 8-week-old mice were cultured in alpha-minimum essential Eagle medium (αMEM) containing 10% fetal bovine serum (FBS), 100 IU/ml penicillin, 100 mg/ml streptomycin, and 100 ng/ml M-CSF on plastic petri dishes. After 3 days of culture, BMMs were seeded at a density of $3 \times 10^4/cm^2$ and cultured in αMEM containing 10% FBS with 100 ng/ml RANKL and 30 ng/ml M-CSF for the indicated days.

CRISPR-Cas9 knockout of MGP gene. Single guide RNA (sgRNA) targeting the mouse *Mgp* gene were designed and synthesized. The selected gRNA exhibiting over 80% inhibition, is targeting to a 20-base sequence (5′-TTGCCACGGCCAGCGCAGCC-3′) in exon 1 of the mouse *Mgp* gene. The lentivirus system for CRISPR-Cas9 includes LentiCRISPRv2 backbone vector (Addgene, 52961), packaging plasmids psPAX2 (Addgene, 12260), and pVSVg (Addgene, 8454). sgRNA oligonucleotides were annealed and ligated into the LentiCRISPRv2 vector, generating plasmids that expressed a gRNA targeting MGP or a nontargeting sgRNA, respectively. Then, HEK-293T cells at 70% confluence were transfected with 1 μg of backbone vector, 750 ng of psPAX2, and 250 ng of pVSVg using Lipofectamine 2000 (Invitrogen). At 12 h after transfection, the medium was changed. Cells were cultured for an additional 36 h before the culture medium was harvested. Once target cells (BMMs or RAW 264.7 cells, as indicated) reached 50% confluence, they were incubated with virus-containing medium for 48 h and further selected in medium containing 2 μg/ml of puromycin (Invitrogen) for an additional 3 days before validation of the knockout efficiency and the following experiments. For the RAW 264.7 cells, fresh selective medium was added every other day for 3 weeks. Single colonies were then picked up, expanded, and examined for knockout efficiency. One clone with the lowest gene expression level was maintained.

Overexpression of MGP. Constructs expressing MGP in the pMX retroviral vector were transfected into the PlatE cells. The medium was changed the next day and then harvested and filtered, and BMMs were infected on day 2 in the presence of 30 ng/ml M-CSF and 4 mg/ml Polybrene (Sigma). After 24 h, cells were selected with 1 μg/ml blastocidin at least for 3 days before being used as osteoclast precursors.

RNA extraction and quantitative PCR. Total RNA was extracted from samples using TRIzol reagent (Invitrogen) according to the manufacturer's instructions. Complementary DNA was synthesized using a SuperScript II first-strand synthesis system (Invitrogen). A 20-μl reaction mixture was prepared, containing 1 μl of complementary DNA, 10 μl of SYBR green PCR master mix (TaKaRa), and 200 nM concentrations of each primer. The $2^{-\Delta\Delta CT}$ method was used for relative quantification of each target, and GAPDH (glyceraldehyde-3-phosphate dehydrogenase) was used as an endogenous control.

Nuclear and cytoplasmic fractionation. Nuclear and cytoplasmic fractionations were separated using NE-PER nuclear and cytoplasmic extraction reagents (Thermo). Briefly, cells were harvested and incubated with ice-cold CER I on ice for 10 min. Then, ice-cold CER II was added, followed by incubation on ice for another 5 min. After centrifugation at 12,000 rpm for 5 min, the supernatant was transferred to a new tube. This was the cytoplasmic fraction. The pellet was suspended with ice-cold NER and vortexed on the highest setting for 15 s every 10 min for a total of 40 min. After centrifugation at 12,000 rpm for 5 min, the supernatant was collected as the nuclear fraction.

Western blotting. Cells were harvested in ice-cold radioimmunoprecipitation assay buffer (20 mM Tris-HCl [pH 7.5], 150 mM NaCl, 1 mM EDTA, 1 mM EGTA, 1% Triton X-100, 2.5 mM sodium pyrophosphate, 1 mM β-glycerophosphate, 1 mM Na_3VO_4, 1 mM NaF, 1$\times$ protease inhibitor mixture; Roche). After quantification using a bicinchoninic acid (BCA) protein assay (Pierce), the cell lysates were subjected to SDS-PAGE and immunoblotting analysis with the indicated primary antibodies and corresponding peroxidase-conjugated secondary antibodies (Jackson ImmunoResearch). Signals were developed using Hyglo chemiluminescent reagent (Thermo) and detected using a ChemiDoc MP (Bio-Rad).

TRAP staining and TRAP assay. Cells were fixed with 4% paraformaldehyde, and tartrate-resistant acid phosphatase (TRAP) staining was performed using a commercial kit (Sigma) according to manufacturer's instructions. The TRAP-positive multinucleated cells (at least three nuclei) in each well were counted. For the TRAP assay, cells were incubated with lysis buffer (90 mM citrate buffer, 80 mM sodium tartrate, 0.1% Triton X-100) for 10 min at room temperature, followed by incubation in substrate solution (20 mM 4-nitrophenyl phosphate) at 37°C for 20 min. The reaction was terminated by 0.5 M NaOH, and the absorbance was read at 415 nm.

Actin ring staining and pit formation assay. BMMs were seeded on bone slices and induced with osteoclastic medium for 4 days. The osteoclasts were fixed with 4% paraformaldehyde and stained with fluorescein isothiocyanate (FITC)-phalloidin at room temperature for 1 h. The pictures of visualize actin rings were captured using a fluorescence microscope. For the pit formation assay, bone slices were incubated in 0.5 N NaOH for 2 min, and the cells were scraped off using a cotton swab. The bone slices were then incubated with 20 mg/ml peroxidase-conjugated wheat germ agglutinin (Sigma) for 30 min. After being washed with phosphate-buffered saline (PBS), the bone slices were exposed to 3,30-diaminobenzidine tablets (Sigma) for 15 min to visualize the pits.

Animal treatments. Cre-dependent FLEX-On recombinant AAVs (serotype rAAV9) were acquired from ViGene Biosciences. The Cre-dependent FLEX-On inducible design can detect restricted tissue-specific expression. In the FLEX-ON system, the gene is in reverse orientation downstream of the

promoter, and the gene is flanked by two oppositely orientated loxPs. In the absence of Cre the gene cannot be expressed, and in the presence of Cre gene expression can be turned on or induced. Each of the virus samples was prepared using a triple-plasmid approach. The main MGP recombinant plasmid or control plasmid, the Rep/Cap plasmid, and the helper plasmid were transfected into HEK293 cells for the packaging of rAAV. After HEK293 cell lysis, rAAV particles were purified by CsCl gradient ultracentrifugation. All of the animal experiment procedures were performed in accordance with National Institutes of Health guidelines for the care and use of laboratory animals and the Xi'an Jiaotong University Animal Care and Use Committee. Eight-week-old LysM Cre male mice were housed in a facility with stable humidity and temperature and a 12-h light-dark cycle. Mice were intratibially injected with recombinant MGP rAAV (2×10^{11} virus genomes [vg]) or control rAAV. Eight weeks later, the mice were euthanized, and blood was collected for serological examination according to the manufacturer's instructions (Shanghai Haling Biotechnology). Bone analysis was performed as described earlier (23).

Microcomputed tomography. Mouse femurs were fixed in 10% neutral buffered formalin prior to scanning. μCT scanning was performed using a Scanco model 35 (Scanco Medical). The trabecular bone samples ranging from just proximal to the distal growth plate to 20% of the bone length were analyzed. The output variables included the total volume (TV), the bone volume (BV), the bone volume/total volume fraction (BV/TV), the trabecular number (TbNo), the trabecular thickness (TbTh), the trabecular spacing (TbSp), and the specific bone surface (BS/BV).

Histology and histomorphometry. Mouse femurs were fixed in 10% neutral buffered formalin, followed by decalcification in 14% EDTA for 2 weeks. The femurs were paraffin embedded, sectioned, and stained using TRAP. The histomorphometric parameters were measured by using a BioQuant OsteoII (BioQuant Image Analysis Corp.) in a blinded fashion. ImageJ software was used to measure the osteoclasts to quantify the osteoclast surface/bone surface (OcS/BS), as previously described (24).

Calcium measurement. Wide-type or $MGP^{-/-}$ RAW 264.7 cells were loaded with 1 μM Fluo-2 (Keygentec) in 10% αMEM at 37°C for 1 h in the dark. The cells were then fully washed with PBS, and reincubated with fresh medium for 30 min. Fluo-2 signals were measured by excitation at 488 nm and emission at 520 nm every 5 s for 10 min. For the RANKL-treated groups, the medium was replaced with 10% αMEM containing 100 ng/ml RANKL at 180 s, and the signal was detected immediately. Each condition was examined using three replicates.

Statistical analyses. Statistical analyses were performed using an unpaired two-tailed Student *t* test. All data are expressed as means ± the standard errors of the mean unless indicated otherwise. The results are representative of more than three independent experiments.

ACKNOWLEDGMENTS

This study was supported by the National Natural Science Foundation of China (no. 81670806 and 81300716), the Fundamental Research Funds for the Central Universities (no. xzy012019094), and the Natural Science Basic Research Project of Shaanxi Province (No. 2017JM8015).

We declare that we have no conflict of interest.

REFERENCES

1. Cancela ML, Laizé V, Conceição N. 2014. Matrix Gla protein and osteocalcin: from gene duplication to neofunctionalization. Arch Biochem Biophys 561:56–63. https://doi.org/10.1016/j.abb.2014.07.020.
2. Luo G, Ducy P, McKee MD, Pinero JP, Loyer E, Behringer RR, Karsenty G. 1997. Spontaneous calcification of arteries and cartilage in mice lacking matrix Gla protein. Nature 386:78–81. https://doi.org/10.1038/386078a0.
3. Schurgers LJ, Spronk HM, Skepper JN, Hackeng TM, Shanahan CM, Vermeer C, Weissberg PL, Proudfoot D. 2007. Posttranslational modifications regulate matrix Gla protein function: importance for inhibition of vascular smooth muscle cell calcification. J Thromb Haemost 5:2503–2511. https://doi.org/10.1111/j.1538-7836.2007.02758.x.
4. Hofbauer LC, Brueck CC, Shanahan CM, Schoppet M, Dobnig H. 2007. Vascular calcification and osteoporosis-from clinical observation towards molecular understanding. Osteoporos Int 18:251–259. https://doi.org/10.1007/s00198-006-0282-z.
5. Kaipatur NR, Murshed M, McKee MD. 2008. Matrix Gla protein inhibition of tooth mineralization. J Dent Res 87:839–844. https://doi.org/10.1177/154405910808700907.
6. Silaghi CN, Fodor D, Cristea V, Crăciun AM. 2011. Synovial and serum levels of uncarboxylated matrix Gla protein (ucMGP) in patients with arthritis. Clin Chem Lab Med 50:125–128. https://doi.org/10.1515/CCLM.2011.713.
7. Misra D, Booth SL, Crosier MD, Ordovas JM, Felson DT, Neogi T. 2011. Matrix Gla protein polymorphism, but not concentrations, is associated with radiographic hand osteoarthritis. J Rheumatol 38:1960–1965. https://doi.org/10.3899/jrheum.100985.
8. Tuñón-Le Poultel D, Cannata-Andía JB, Román-García P, Díaz-López JB, Coto E, Gómez C, Naves-Díaz M, Rodríguez I. 2014. Association of matrix Gla protein gene functional polymorphisms with loss of bone mineral density and progression of aortic calcification. Osteoporos Int 25:1237–1246. https://doi.org/10.1007/s00198-013-2577-1.
9. Yagami K, Suh JY, Enomoto-Iwamoto M, Koyama E, Abrams WR, Shapiro IM, Pacifici M, Iwamoto M. 1999. Matrix GLA protein is a developmental regulator of chondrocyte mineralization and, when constitutively expressed, blocks endochondral and intramembranous ossification in the limb. J Cell Biol 147:1097–1108. https://doi.org/10.1083/jcb.147.5.1097.
10. Gopalakrishnan R, Suttamanatwong S, Carlson AE, Franceschi RT. 2005. Roe of matrix Gla protein in parathyroid hormone inhibition of osteoblast mineralization. Cells Tissues Organs 181:166–175. https://doi.org/10.1159/000091378.
11. Amarasekara DS, Yun H, Kim S, Lee N, Kim H, Rho J. 2018. Regulation of osteoclast differentiation by cytokine networks. Immune Netw 18:e8. https://doi.org/10.4110/in.2018.18.e8.
12. Kajiya H. 2012. Calcium signaling in osteoclast differentiation and bone resorption. Adv Exp Med Biol 740:917–932. https://doi.org/10.1007/978-94-007-2888-2_41.
13. Newman B, Gigout LI, Sudre L, Grant ME, Wallis GA. 2001. Coordinated expression of matrix Gla protein is required during endochondral ossification for chondrocyte survival. J Cell Biol 154:659–666. https://doi.org/10.1083/jcb.200106040.
14. Julien M, Khoshniat S, Lacreusette A, Gatius M, Bozec A, Wagner EF, Wittrant Y, Masson M, Weiss P, Beck L, Magne D, Guicheux J. 2009. Phosphate-dependent regulation of MGP in osteoblasts: role of ERK1/2

and Fra-1. J Bone Miner Res 24:1856–1868. https://doi.org/10.1359/jbmr.090508.
15. Marulanda J, Gao C, Roman H, Henderson JE, Murshed M. 2013. Prevention of arterial calcification corrects the low bone mass phenotype in MGP-deficient mice. Bone 57:499–508. https://doi.org/10.1016/j.bone.2013.08.021.
16. Rachner TD, Khosla S, Hofbauer LC. 2011. Osteoporosis: now and the future. Lancet 377:1276–1287. https://doi.org/10.1016/S0140-6736(10)62349-5.
17. Vassalle C, Mazzone A. 2016. Bone loss and vascular calcification: a bidirectional interplay? Vascul Pharmacol 86:77–86. https://doi.org/10.1016/j.vph.2016.07.003.
18. El-Maadawy S, Kaartinen MT, Schinke T, Murshed M, Karsenty G, McKee MD. 2003. Cartilage formation and calcification in arteries of mice lacking matrix Gla protein. Connect Tissue Res 44:272–278. https://doi.org/10.1080/03008200390181762.
19. Zou W, Kitaura H, Reeve J, Long F, Tybulewicz VL, Shattil SJ, Ginsberg MH, Ross FP, Teitelbaum SL. 2007. Syk, c-Src, the $\alpha v\beta 3$ integrin, and ITAM immunoreceptors, in concert, regulate osteoclastic bone resorption. J Cell Biol 176:877–888. https://doi.org/10.1083/jcb.200611083.
20. Nishimoto SK, Nishimoto M. 2005. Matrix Gla protein C-terminal region binds to vitronectin: colocalization suggests binding occurs during tissue development. Matrix Biol 24:353–361. https://doi.org/10.1016/j.matbio.2005.05.004.
21. Coen G, Ballanti P, Silvestrini G, Mantella D, Manni M, Di Giulio S, Pisanò S, Leopizzi M, Di Lullo G, Bonucci E. 2009. Immunohistochemical localization and mRNA expression of matrix Gla protein and fetuin-A in bone biopsies of hemodialysis patients. Virchows Arch 454:263–271. https://doi.org/10.1007/s00428-008-0724-4.
22. Faccio R, Zou W, Colaianni G, Teitelbaum SL, Ross FP. 2003. High-dose M-CSF partially rescues the Dap12$^{-/-}$ osteoclast phenotype. J Cell Biochem 90:871–883. https://doi.org/10.1002/jcb.10694.
23. Zhang Y, Su J, Wu S, Teng Y, Yin Z, Guo Y, Li J, Li K, Yao L, Li X. 2015. DDR2 (discoidin domain receptor 2) suppresses osteoclastogenesis and is a potential therapeutic target in osteoporosis. Sci Signal 248(369):ra3.
24. Zhang Y, Rohatgi N, Veis DJ, Schilling J, Teitelbaum SL, Zou W. 2018. PGC1β organizes the osteoclast cytoskeleton by mitochondrial biogenesis and activation. J Bone Miner Res 33:1114–1125. https://doi.org/10.1002/jbmr.3398.